Modeling the optical constants of wide bandgap materials

Aleksandra B. Djurišić [a], Kwok-On Tsang [b], and E. Herbert Li [b*]
[a] Institut for Applied Photophysics, University of Technology Dresden, Mommsenstr. 13
D-01069 Dresden, Germany
[b] Department of Electrical and Electronic Engineering, University of Hong Kong
Pokfulam Road, Hong Kong

ABSTRACT

Calculations of the optical constants of hexagonal GaN (in the range 1-10 eV), InN (in the range 2-20 eV), AlN (in the range 6-20 eV) and 6H-SiC (in the range 1-30 eV) for the component perpendicular to the *c* axis are presented. The employed model is modified Adachi's model of the optical properties of semiconductors. In the employed model, damping constant Γ describing broadening phenomenon is replaced with the frequency dependent expression $\Gamma(\omega)$. In such a manner, type of broadening represents adjustable parameter of the model, allowing broadening to vary over a range of functions with similar kernels but different wings. Excellent agreement with experimental data is obtained for all investigated materials. Obtained relative rms errors for the real and imaginary parts of the index of refraction are equal to 3.5% and 5.2% for 6H-SiC in the 1-30 eV range, 1.7% and 4.1% for GaN in the 1.5-10 eV range, 1.2% and 2.5% for InN in the 2-10 eV range and 1.5% and 1.9% for AlN in the 6-20 eV range.

Keywords: optical constants, semiconductors

1. INTRODUCTION

Wide band gap semiconductors, such as III-V nitrides, have attracted much attention because of their potential use in optoelectronic device applications in visible and near UV range [1]. Silicon carbide is also a wide band gap semiconductor, which has received much attention recently, especially since the release of commercial 6H-SiC bulk substrates in 1991 and 4H-SiC substrates in 1994 [2]. The nitrides are characterized by high ionicity, very short bond lengths, low compressibility and high thermal conductivity. They usually crystallize in the hexagonal form, though successful growth of zinc-blende forms has been reported recently. Since the fundamental band-gaps of hexagonal InN, GaN and AlN are around 1.9 eV, 3.5 eV and 6.2 eV, respectively, their ternary systems are interesting for electroluminescence devices operating at wavelengths from orange to ultraviolet [3]. Silicon carbide is characterized by a high saturation electron drift velocity, thermal conductivity and breakdown field. It forms over a hundred different polytypes [4], which polytypes are divided into three basic crystallographic categories; cubic (C), hexagonal (H) and rhombohedral (R). In the SiC polytypes individual bond lengths are nearly identical, and polytypes are differentiated by the stacking sequence of each tetrahedrally bonded Si-C bilayer. All polytypes have indirect band gap, whose values range from 2.42 eV for cubic 3C-SiC to 3.33 eV for hexagonal 2H-SiC [5]. Among the various polytypes, the 6H modification is the one most extensively studied. It consists of two-thirds cubic and one-third hexagonal bonds, but the overall symmetry of the crystal is hexagonal. 6H-SiC has band gap in the blue spectral region (about 2.86-3.02 eV [5,6]) and its applications in light-emitting optoelectronic devices are possible [7]. Also, it is frequently used as a substrate for the nitride films since the lattice mismatch is only 1% for AlN [8] and 3% for GaN [9].

In the design of optoelectronic devices, such as lasers and waveguide devices, interplay between the physical dimensions of the device and the index of refraction requires the index of refraction to be known as a function of wavelength as precisely as possible. Furthermore, in experimental determination of the optical constants, such as spectroscopic ellipsometry, it is required to know optical properties of all other layers and the substrate in order to acquire optical constants of the investigated layer. Since 6H-SiC is often used as a substrate for the nitride films growth, and buffer layers of binary nitride materials are often used to improve characteristics of the film [10], there is considerable interest in the optical properties of

* Email:ehli@eee.hku.hk; http://www-herbert.eee.hku.hk; tel: +852 2859 7091; fax: +852 2559 8738

these materials. It is well known that the optical properties of solids can be described in terms of the complex dielectric function $\varepsilon(\omega) = \varepsilon_1(\omega) + i\varepsilon_2(\omega)$ or the complex index of refraction $N(\omega) = n(\omega) + ik(\omega)$.

There have been several experimental studies of optical constants of GaN [11-13], InN [14], AlN [15-17] and 6H-SiC [18-21]. However, experimental dielectric function data are not expressed as analytical functions of critical point energies or photon energy. This deficiency can be overcome by modeling. The model for the index of refraction should be simple and concise, but complex enough to account for all the relevant features of the index of refraction over wide energy range. One of the frequently employed models for the optical constants of solids is the one of Adachi [11,22]. Adachi's model dielectric function (MDF) is a relatively simple model which describes the dielectric function with terms corresponding to transitions at major critical points in the joint density of states (E_0, $E_0+\Delta_0$, E_1, $E_1+\Delta_1$,E_0',$E_2(X)$, and $E_2(\Sigma)$ for the zinc-blende structure [22] and E_0, E_{1A}, E_{1B}, and E_{1C} for the hexagonal structure [11]). We present here calculations of the optical constants corresponding to the component perpendicular to the c axis (there are no available experimental data for the parallel polarization) for hexagonal GaN, InN, AlN and 6H-SiC.

In this work, the MDF is augmented by replacing the damping constant Γ describing broadening phenomenon with the frequency dependent expression $\Gamma(\omega)$, so that simplicity of the model equations is retained, while accuracy, especially around fundamental band gap E_0 region, is improved. Frequency dependent damping $\Gamma(\omega)$ allows broadening to vary over a range of functions with similar kernels and different wings. Since type of broadening is an adjustable model parameter, overestimation of the absorption in the vicinity of the fundamental band gap, inherent to the conventional Lorentzian broadening due to wide wings of the Lorentzian function, can be avoided. It has been shown that the broadening caused by electron-phonon and electron-impurities scattering can be described by Gaussian broadening function [23]. However, Lorentzian broadening assumption is commonly used because the assumption of the Gaussian broadening does not give the expression for the dielectric function analytically in a closed form. Frequency dependent damping has important advantage over both Lorentzian and Gaussian broadening: it can mimic closely the Gaussian lineshape which in certain cases more accurately describes the broadening mechanism while it gives analytical solutions, and type of broadening is adjustable, it is not set *a priori*. In such a manner, greater flexibility of the model is achieved, enabling us to obtain excellent agreement with experimental data for both materials in the entire investigated spectral range.

2. DESCRIPTION OF THE MODEL

The complex dielectric function is described by the sum of one-electron and excitonic terms at critical points E_0 and $E_{1\beta}$, $\beta =$ A, B,C and the additive constant ε_∞. The contribution of the E_0 gap is given by:

$$\varepsilon_0(E) = AE_0^{-3/2}\chi_0^{-2}\left[2-(1+\chi_0)^{1/2}-(1-\chi_0)^{1/2}\right], \quad (1)$$

where

$$\chi_0 = \frac{E+i\Gamma_0}{E_0}. \quad (2)$$

A and Γ_0 are the strength and damping constant of the E_0 transition, respectively. Exciton contributions at E_0 critical point are given by

$$\varepsilon_{0X}(E) = \sum_{m=1}^{\infty}\frac{A_0^{ex}}{m^3}\frac{1}{E_0-(G_0^{3D}/m^2)-E-i\Gamma_0}, \quad (3)$$

where A_0^{ex} is the 3D exciton strength parameter, and G_0^{3D} is the 3D exciton binding energy.

Contributions of the critical points $E_{1\beta}$ are given by:

$$\varepsilon_1(E) = -\sum_{\beta=A,B,C} B_{1\beta}\chi_{1\beta}^{-2}\ln(1-\chi_{1\beta}^2), \quad (4)$$

where

$$\chi_{1\beta} = \frac{E+i\Gamma_{1\beta}}{E_{1\beta}}, \quad (5)$$

while $B_{1\beta}$ and $\Gamma_{1\beta}$ are the strengths and the damping constants of the $E_{1\beta}$ transitions respectively. Contributions of the Wannier type 2D excitons (discrete series of exciton lines at the $E_{1\beta}$ critical points) are given by

$$\varepsilon_{1X}(E) = \sum_{\beta=A,B,C} \sum_{m=1}^{\infty} \frac{B_{1\beta}^{X}}{(2m-1)^3} \frac{1}{E_{1\beta} - (G_{1\beta}^{2D}/(2m-1)^2) - E - i\Gamma_{1\beta}}, \tag{6}$$

where $B_{1\beta}^{X}$ and $G_{1\beta}^{2D}$ are the strengths and binding energies of the excitons at $E_{1\beta}$ respectively.

The fact that Lorentzian broadening fails to describe accurately absorption processes, especially in E_0 critical point region, has already been recognized [23-26]. It was shown that by replacing the damping constant Γ_j with the frequency dependent expression, better agreement with experimental data can be achieved for both models of Kim *et al.* [23] and of Adachi [24] for the zincblende semiconductors. Therefore, in the model for hexagonal semiconductors employed here we replace damping constants Γ_j ($j = 0, 1A, 1B, 1C$) in equations (1)-(6) with the expression

$$\Gamma_j'(E) = \Gamma_j \exp\left[-\alpha_j \left(\frac{(E - E_j)}{\Gamma_j}\right)^2\right]. \tag{7}$$

In such a manner, the broadening function can vary over a range of functions with similar kernels and different wings. Therefore, overestimation of the absorption in the vicinity of a critical point can be avoided, without any initial assumption about the broadening type for the transitions at that critical point.

The dielectric function for GaN, InN and AlN is then given by $\varepsilon(E) = \varepsilon_0(E) + \varepsilon_{0X}(E) + \varepsilon_1(E) + \varepsilon_{1X}(E) + \varepsilon_\infty$, while for 6H-SiC the term $\varepsilon_0(E)$ given by Eq. (1) is left out. Since 6H-SiC exhibits pronounced excitonic effects around E_0 critical point [27], we have disregarded the contribution of the indirect interband transition to the dielectric function. Inclusion of this transition, which represents a second order perturbation and hence it is very weak, would only increase number of employed model parameters, without being justified by improving the agreement with experimental data. When the dielectric function is known, real and imaginary parts of the index of refraction are readily calculated from the formulae

$$n(\omega) = \left[0.5\left(\varepsilon_1(\omega) + \left(\varepsilon_1^2(\omega) + \varepsilon_2^2(\omega)\right)^{1/2}\right)\right]^{1/2} \tag{8}$$

and

$$k(\omega) = \left[0.5\left(-\varepsilon_1(\omega) + \left(\varepsilon_1^2(\omega) + \varepsilon_2^2(\omega)\right)^{1/2}\right)\right]^{1/2}. \tag{9}$$

3. RESULTS AND DISCUSSION

Model parameters were determined using acceptance-probability-controlled simulated annealing algorithm [28,29], by minimizing the following objective function

$$F = \sum_{i=1}^{N} \left[\left|\frac{n(\omega_i) - n^{expt}(\omega_i)}{n^{expt}(\omega_i)}\right| + \left|\frac{k(\omega_i) - k^{expt}(\omega_i)}{k^{expt}(\omega_i)}\right|\right], \tag{10}$$

where $n(\omega_i), n^{expt}(\omega_i)$, respectively, are the calculated and the experimental values of the real part, and $k(\omega_i), k^{expt}(\omega_i)$ are the calculated and the experimental values of the imaginary part of the index of refraction at frequency ω_i. The employed algorithm is a global optimization routine, i.e. obtained result does not depend on the initial estimates which are difficult to provide for all the parameters except the energies of critical points. The objective function given by Eq. (10) provides that the discrepancies between the calculated and experimental values for both the real and imaginary parts of the index of refraction are minimized at the same time. We choose to fit the refractive index, which gives lower magnitude of change in the objective function. Since certain parameters of the employed algorithm strongly depend on the magnitude of change in the objective function, such a choice of an objective function provides improved numerical stability of the algorithm.

Obtained values of model parameters are given in Table I. Fig. 1 shows the real and imaginary parts of the dielectric function of hexagonal GaN as a function of energy. The open circles represent experimental data, solid line is the dielectric function calculated using the model presented here, while the broken line represents the results of Kawashima *et al.* [11] who used the conventional MDF. As an indication of the accuracy with respect to the experimental values, we have

calculated relative rms errors for the real and imaginary parts of the index of refraction. For our calculations, those errors equal 1.7% and 4.1% for the real and imaginary parts of the index of refraction, respectively, while rms errors for the results of Kawashima *et al.* Equal 7.4% for n and 22.8 for k. It can be observed that our model is clearly superior over the conventional MDF. . Fig. 2 depicts the real and imaginary parts of dielectric function of hexagonal InN as a function of energy. In this case, relative rms errors equal 1.2% for n and 2.5 for k. Fig. 3 shows the real and imaginary parts of dielectric function of hexagonal AlN as a function of energy. Relative rms errors equal 1.5% for the real part and 1.9% for the imaginary part of the index of refraction. Fig. 4 shows the real and imaginary part of the dielectric function of 6H-SiC *vs.* energy. Relative rms errors for the real and imaginary parts of the index of refraction are 3.5% and 5.2% respectively. Excellent agreement of our calculations with the experimental data can be observed for all four materials. The parameters Γ_0 and α_0 given in Table I for all investigated materials correspond to a broadening function closer to the Gaussian one than to Lorentzian one, i.e. there is no excessive absorption inherent to models with Lorentzian broadening due to the large wings of broadening function. Therefore, it can be concluded that the absorption at the fundamental band gap exhibits broadening which cannot be adequately described with the conventional Lorentzian broadening assumption. For other critical points, however, no conclusion valid for al materials can be drawn.

Table I. Model parameter values

par.	GaN	InN	AlN	6H-SiC
ε_∞	0.426	1.314	1.230	1.650
A ($eV^{1.5}$)	41.251	12.256	5.648	---
α_0	1.241	5.345	0.465	1.502
Γ_0 (eV)	0.287	0.037	0.439	0.045
E_0 (eV)	3.550	2.247	6.222	2.990
B_{1A}	0.778	0.361	0.236	1.516
B_{1B}	0.103	1.074	0.037	0.001
B_{1C}	0.920	0.007	0.230	0.002
B_{1A}^X (eV)	2.042	1.243	1.393	0.001
B_{1B}^X (eV)	1.024	0.471	1.655	11.397
B_{1C}^X (eV)	1.997	5.528	3.234	6.437
α_{1A}	0.240	5.161	0.747	7.755
α_{1B}	0.011	0.574	0.687	0.196
α_{1C}	0.005	1.108	1.913	1.073
Γ_{1A} (eV)	0.743	0.052	0.064	1.488
Γ_{1B} (eV)	0.428	0.012	2.045	0.849
Γ_{1C} (eV)	0.440	2.698	0.411	4.493
G_{1A}^{2D} (eV)	0.0003	1.148	2.880	6.273
G_{1B}^{2D} (eV)	0.356	0.521	0.980	0.191
G_{1C}^{2D} (eV)	1.962	4.801	5.507	4.298
E_{1A} (eV)	6.010	6.400	12.055	5.429
E_{1B} (eV)	8.182	8.230	8.841	7.346
E_{1C} (eV)	8.761	7.308	12.900	14.148
G_0^{3D} (eV)	0.030	0.024	0.060	0.037
A_0^{ex} (eV)	0.249	0.001	0.600	0.013

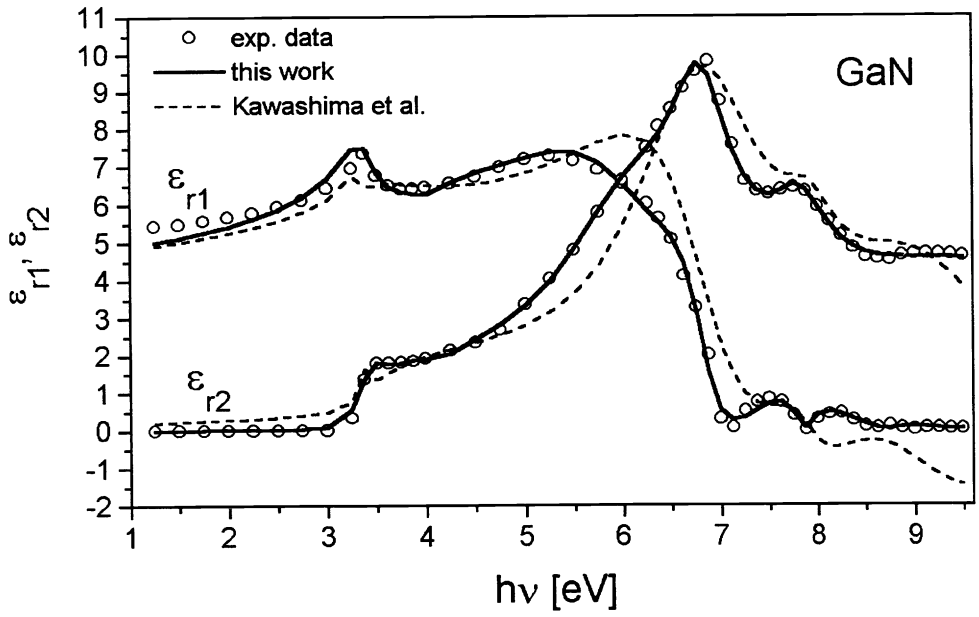

Figure 1. The real and imaginary parts of the dielectric function of GaN *vs.* energy; circles – experimental data, solid line – model, this work; calculations of Kawashima *et al.*.

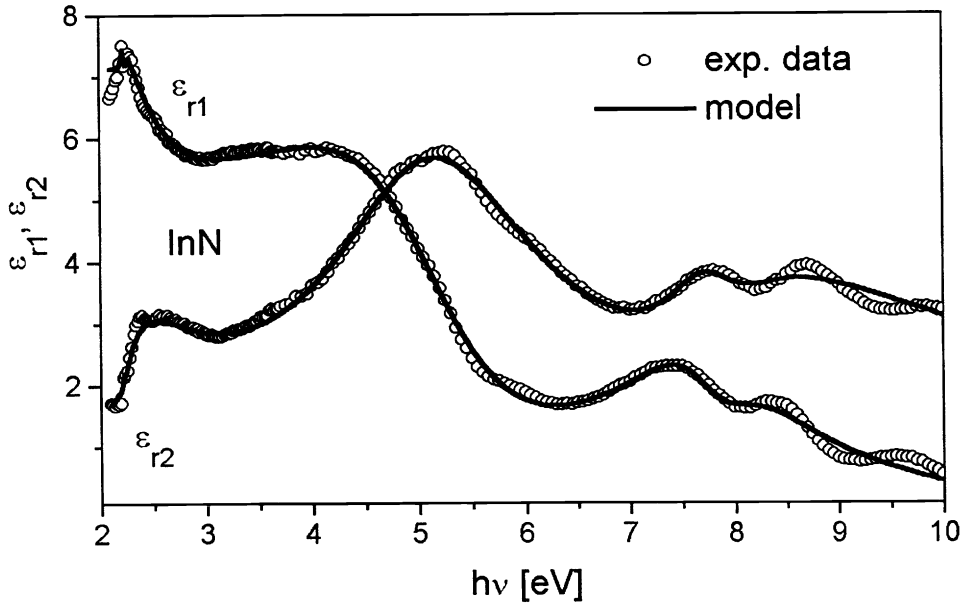

Figure 2. The real and imaginary parts of the dielectric function of InN *vs.* energy; circles – experimental data, solid line – model.

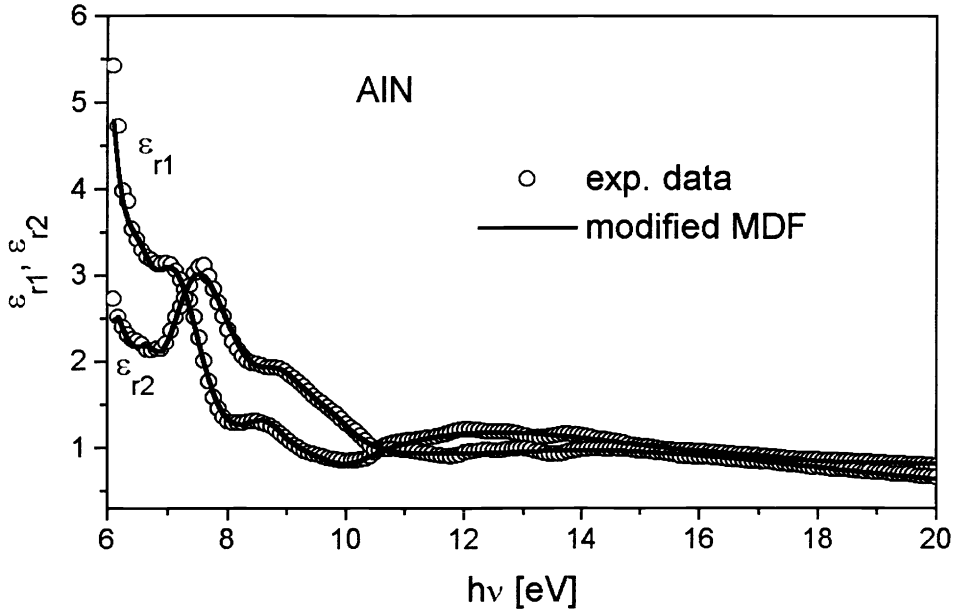

Figure 3. The real and imaginary parts of the dielectric function of AlN *vs.* energy; circles – experimental data, solid line – model.

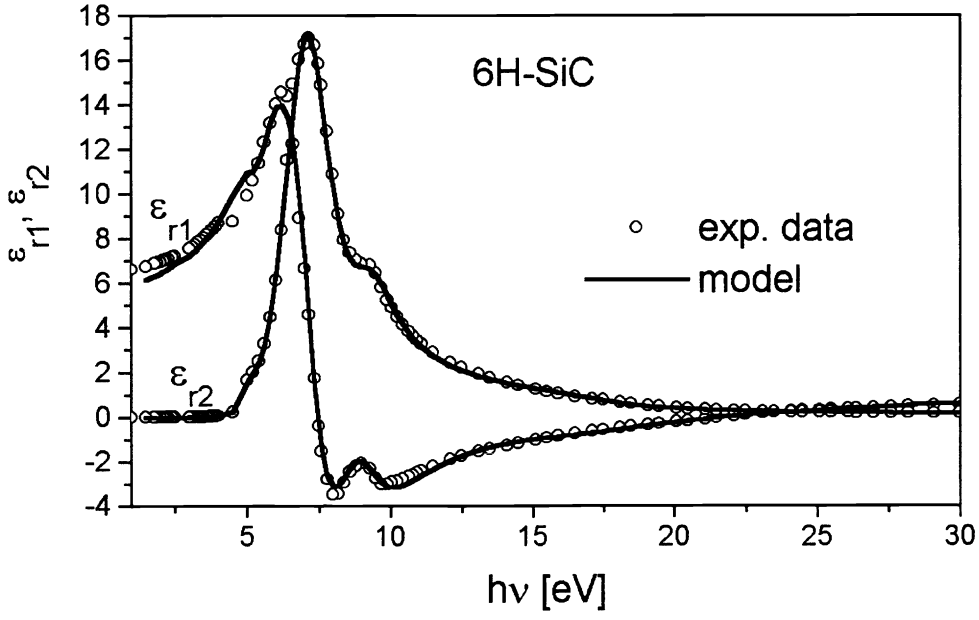

Figure 4. The real and imaginary parts of the dielectric function of 6H-SiC *vs.* energy; circles – experimental data, solid line – model.

4. CONCLUSION

We have obtained excellent agreement between our proposed model and experimental data for the hexagonal GaN, InN, AlN and 6H-SiC over a wide spectral range. The model employs variable broadening instead of the conventional Lorentzian one. Broadening type is determined by the ratio of two adjustable model parameters, so that this model is very flexible since no broadening mechanism is set *a priori*. From the obtained values of model parameters, we conclude that assumption of Lorentzian broadening is not justified in the neighborhood of the fundamental band gap E_0. Obtained relative

rms error for the real part of the index of refraction is below 4% for all investigated materials, while for the imaginary part, it is below 6%.

ACKNOWLEDGEMENTS

This work is supported by the CRCG research grant of the University of Hong Kong. A. B. Djurišić would also like to acknowledge the support of a William Mong Postdoctoral fellowship in the Faculty of Engineering for this work.

REFERENCES

1.S. Nakamura nad G. Fasol, *The blue laser diode: GaN based light emitters and lasers*, Springer, Berlin, (1997).
2. R. Casady and R. W. Johnson,"Status of silicon carbide (SiC) as a wide-bandgap semiconductor for high temperature applications: a review ", *Solid State Commun.* **39**, pp. 1409-1422, 1996.
3. D. W. Jenkins and J. D. Dow, "Electronic structures and doping of IN, $In_xGa_{1-x}N$, and $In_xAl_{1-x}N$", *Phys. Rev. B* **39**, pp. 3317-3329, 1989.
4. G. C. Trigunayat and G. K. Chada, "Progress in the study of polytypism in crystals (I)", *phys. stat. solidi a* **4**, pp. 9 – 42, 1971.
5. in *Numerical Data and Functional Relationships in Science and Technology*, edited by K. H. Hellwege and O. Madelung, Landolt-Bornstein, New Series III, Crystal and solid state physics, vol. 17a, Springer, Berlin, pp.132-141,1987.
6. C. H. Park, B.-H. Cheong, K.-H. Lee and K. J. Chang, "Structural and electronic properties of cubic, 2H, 4H, and 6H SiC", *Phys. Rev. B* **49**, pp. 4485-4493, 1994.
7. P. A. Ivanov and V. E. Chelnokov, "Recent developments in SiC single crystal electronics.", *Semicond. Sci. Technol.* **7**, pp. 863-880, 1992.
8. T. George, W. T. Pike, M. A. Khan, J. N. Kuznia and P. Chang-Chien, "A microstructural comparison of the initial growth of AlN and GaN layers on basal plane sapphire and SiC substrates I Low pressure metalorganic vapor deposition", *J. Electron. Mater.* **24**, pp. 241-247 (1995).
9.W. M. Yim, E. J. Stofko, P. J. Zanzucchi, J. I. Pankove, E. Ettenberg,and S. L. Gilbert, "Epitaxially grown AlN and its optical band gap",*J. Appl. Phys.***44**, pp. 292-297, 1973.
10. I. Akasaki and H. Amano, "Organometallic vapor-phase epitaxy of gallium nitride for high-brightness blue light emitting diodes", G.B. Stringfellow, M. George Craford ed., *Semiconductors and semimetals* **48**, pp. 357-390, Academic Press, San Diego, 1997.
11. T. Kawashima, H. Yoshikawa, S. Adachi, S. Fuke and H. Ohtsuka, "Optical properties of hexagonal GaN", *J. Appl. Phys.* **82**, pp. 3528-3535, 1997.
12. S. Logothetidis, J. Petalas, M. Cardona and T. D. Moustakas,"optical properties and temperature dependence of the interband transitions of cubic and hexagonal GaN", *Phys. Rev. B* **50**, pp. 18017-18029, 1994.
13. C. G. Olson, D. W. Lynch and A. Zehe, "10-30 eV optical properties of GaN", *Phys. Rev. B* **24**, pp. 4629-4633, 1981.
14. Q. Guo, O. Kato, M. Fujisawa and A. Yoshida, "Optical constants of indium nitride", *Solid State Commun.* **83**, pp. 721-723, 1992.
15. H. Yamashita, K. Fukui, S. Misawa and S. Yoshida, "Optical properties of AlN epitaxial thin films in the vacuum ultraviolet region", *J. Appl. Phys.* **50**, pp. 896-898, 1979.
16. Q. Guo, M. Nishio, H. Ogawa and A. Yoshida, "Optical properties of aluminum nitride", *Phys. Rev. B* **55**, pp. R15987-R15988, 1997.
17. S. Loughin, R. H. French, W. Y. Ching, Y. N. Xu and G. A. Slack, "Electronic structure of aluminum nitride: theory and experiment", *Appl. Phys. Lett.* **63**, pp. 1182-1184 , 1993.
18. W. R. L. Lambrecht, B. Segall, M. Yoganathan, W. Suttrop, R. P. Devaty, W. J. Choyke, J. A. Edmond, J. A. Powell and M. Alouani, "Calculated and measured uv reflectivity of SiC polytypes", *Phys. Rev. B* **50**, pp. 10722-10726, 1994.
19. W. J. Choyke and E. D. Palik, in *Handbook of Optical Constants of Solids*, edited by E. D. Palik (Academic Press Inc., Orlando, Fl.), pp. 587-595, 1985.
20. S. Logothetidis and J. Petalas, "Dielectric function and reflectivity of 3C-silicon carbide and the component perpendicular to the c axis of 6H-silicon carbide in the energy region 1.5-9.5 eV", *J. Appl. Phys.* **80**, pp. 1768-1772, 1996.
21. P. T. B. Shaffer, "Refractive index, dispersion, and birefringence of silicon carbide polytypes", *Appl. Opt.* **10**, pp. 1034-1036, 1971.
22. S. Ozaki and S. Adachi, "Spectroscopic ellipsometry and thermoreflectance of GaAs", *J. Appl. Phys.* **78**, pp. 3380-3386, 1995.
23. C.C. Kim, J.W. Garland, H. Abad and P.~M. Raccah, "Modeling the optical dielectric function of semiconductors: extension of the critical-point parabolic-band approximation", *Phys. Rev. B* **45**, pp. 11749-11767, 1992.

24. A.~D. Rakić and M.L. Majewski, "Modeling the optical dielectric function of GaAs and AlAs: extension of Adachi's model", *J. Appl. Phys.* **80**, pp. 5909-5915, 1996.
25. O. Stenzel, R. Petrich, W. Scharff, A. Tikhonravov and V.Hopfe, "A hybrid method for determination of optical thin film constants", *Thin Solid Films* **207**, pp. 324-329, 1992.
26. A. Franke, A. Stendal, O. Stenzel and C. Von Borczyskowski, "Gaussian quadrature approach to the calculation of the optical constants in the vicinity of inhomogenously broadened absorption lines", *Pure Appl. Opt.* **5**, pp. 845-853, 1996.
27. W. J. Choyke and L. Patrick, "Exciton recombination radiation and phonon spectrum of 6H-SiC", *Phys. Rev.* **127**, pp. 1868-1877, 1962.
28. A.D.Rakić, J.M. Elazar and A.B. Djurišić, "Acceptance-probability-controlled simulated annealing: A method for modeling the optical constants of solids", *Phys. Rev. E*, Vol. **52**, pp. 6862--6867, 1995.
29. A. B. Djurišić, J. M. Elazar and A. D. Rakić, "Modeling the optical constants of solids using acceptance-probability-controlled simulated annealing with adaptive move generation procedure", *Phys. Rev. E*, Vol. 55, pp. 4797-4803, 1997.